

---

*Electronic Journal of*  
**SEVERE STORMS METEOROLOGY**

---

**Quantifying the relationships between environmental factors and accumulated tornado energy on the most prolific days in the largest "outbreaks"**

Zoe Schroder and James B. Elsner  
*Florida State University, Tallahassee, FL*

(This is a non-peer reviewed preprint submitted to EarthAxiv)

ABSTRACT

Outbreaks over consecutive days with many tornadoes are typically associated with specific regional scale environmental factors. To quantify the relationship between environmental factors and tornado activity, the authors examine big days in the largest outbreaks. They identify the largest groups across space and time and analyze the days within these groups that have at least ten tornadoes (big days). A climatology of the big days shows that they occur most often during April, May, and June across the central United States. Then, defining accumulated tornado energy (ATE) as a metric of big day severity, they statistically examine how this metric is related to environmental factors including convective available energy and shear using a regression model. They find an upward trend in per big-day outbreak ATE of 7% [(2.5%, 12%), 95% UI] per annum and an increase in ATE of 83% [(23%,170%), 95% UI] for every  $10 \text{ m}^2 \text{ s}^{-2}$  increase in the magnitude of bulk shear. Further, they find an increase of 49% [(18%, 87%), 95% UI] for every  $1000 \text{ J kg}^{-1}$  increase in CAPE. Residuals from the regression model shows no regional difference in where the model over predicts ATE and where the model under predicts ATE. However, the number of tornadoes per unit area is larger on big days where the model under predicts ATE.

---

**1. Introduction**

Tornado outbreaks pose a large risk for significant damage and casualties. For example, the April 27, 2011 outbreak produced 199 tornadoes. It resulted in 316 fatalities, more than 2700 injuries, and insured losses that exceeded \$11 billion (Knupp et al. 2014). The vast majority of tornado-related fatalities occur in outbreaks (Galway 1977; Schneider et al. 2004; Fuhrmann et al. 2014). In fact, three-fourths of all fatalities occur on days with the most tornadoes within a large outbreak.

The climatology of tornado outbreaks is well documented. Outbreaks vary by location, season, and intensity. In general, outbreaks occur east of the Rocky Mountains and west of the Appalachian Mountains (Dean 2010) and are most common in the central and southeastern part of the country with the frequency of occurrence in those areas varying by season.

Tornado outbreaks occur most often during April, May, and June (Galway 1977; Dean 2010). In these months, the majority of outbreaks occur across the Central Plains and the Southeast. Outbreaks become less common in the Southeast and the Southern Plains during the summer months because of the northern migration of the jet stream (Concannon et al. 2000). Outbreaks are largely confined to the Southeast during the late fall and winter months (Dean 2010). For example, the November 23 - 24, 2004 outbreak extended from Texas to Florida and Georgia. It produced 93 tornadoes resulting in 42 casualties.

Missing from these studies is a quantification of the relationship between environmental factors and collective tornado activity. Specifically, how much convective energy is needed, on average, to produce a 25% increase in tornado activity? Tornado environments have been studied locally using proximity soundings

and local weather stations. A proximity sounding is a measure of atmospheric variables such as temperature, pressure, and winds for a specific location and time. These studies have identified environmental factors important to the development of tornadoes such as convective available potential energy (CAPE), speed and directional wind shear, and low cloud-base heights (Brooks et al. 1994; Jackson and Brown 2009; Brown 2002; Craven et al. 2002). The amount of CAPE and wind shear varies by event and geographic region. A tornado can form in low CAPE with high shear environments and high CAPE with low shear environments (Johns et al. 1993; Korotky et al. 1993; Brooks et al. 1994). Here we are interested in how much tornado activity changes with a unit change in CAPE controlling for wind shear.

The objective of the present study is to quantify the extent to which environmental factors modulate collective tornado activity. We first identify the biggest days in the largest groups. We then determine which environmental factors, individually and interactively, best explain cumulative tornado activity. The metric of cumulative activity is accumulated tornado energy and the environmental variables we consider include convective available potential energy, convective inhibition, helicity, and bulk shear.

The paper is outlined as follows. In section 2, we describe the method we use to define tornado groups, and we compare the resulting list of significant large groups with previous lists of significant outbreaks. We also introduce the metric of accumulated tornado energy (ATE) In section 3, we describe some of the spatial and temporal characteristics of the biggest days in the largest groups. Additionally, we quantify the relationship between ATE and the environmental variables using regression models. In section 4, we provide a summary and list the main conclusions.

---

*Corresponding author address:* Zoe Schroder, Department of Geography, Florida State University, 113 Collegiate Loop, Tallahassee, FL 32301, E-mail: [zms17b@my.fsu.edu](mailto:zms17b@my.fsu.edu)

## 2. Methods

A tornado can occur as a single isolated event or as one of several to dozens within an outbreak. The American Meteorological Society

formally defines a tornado outbreak as “multiple tornado occurrences associated with a particular synoptic-scale system” (American Meteorological Society cited 2018). A tornado outbreak can occur over a time span ranging from as short as an hour to as long as several days. Less formally, it is commonly understood that an outbreak is a group of several to hundreds of tornadoes that occur within a relatively short time scale and over a limited geographic region (Malamud et al. 2016). Here we focus on tornado groups rather than on individual tornadoes because tornado groups have a spatial and temporal extent that is associated with synoptic-scale environmental parameters. We refer to them as a group rather than an outbreak since we make no attempt to associate them with a particular synoptic-scale system (e.g., an extra-tropical cyclone).

### *a. Grouping tornadoes*

We obtain tornado data from the Storm Prediction Center’s extensive tornado record (<https://www.spc.noaa.gov/wcm/#data>). Date, time, and location of each tornado are used to delineate groups of tornadoes. The data are subset to include only tornadoes that occur from 1994 to 2017 in the contiguous United States. The start year of 1994 marks the beginning of the extensive use of the WSR-88D radar. There are 29,372 tornadoes over this period of record.

We first project the geographic coordinates of the tornado locations using a Lambert Conic Conformal projection for the contiguous United States. The origin of the projection is situated in eastern Kansas at 39 degrees North and 96 degrees West. Then for a given tornado location  $i$ , we compute the Euclidean distance ( $d_{ij}$ ) as the difference between location  $i$  and the location of tornado  $j$ . Similarly we compute a time difference ( $t_{ij}$ ) between the time of tornado  $i$  and the time of tornado  $j$ . The space difference has units of meters and the time difference has units of seconds. The space difference is divided by ten so the magnitude is commensurate with the corresponding time difference under the assumption that, on average, thunderstorms move at ten meters per second. For every tornado pair, the space and time differences are added to give a total space-time difference (Eq. 1).

$$\delta_k = d_{ij} + t_{ij}, \quad (1)$$

where  $k = n(n + 1) / 2$  indexes the unique

tornado pairs and  $n$  is the number of tornadoes.

Next, the set of  $k$  space-time differences ( $\delta_k$ ) is used to place each tornado into a group. If tornado  $i$  is in close proximity to tornado  $j$  based on a small  $\delta_k$ , then the two tornadoes are considered in the same group. Grouping is done using the single-linkage method whereby the two tornadoes with the smallest  $\delta_k$  are grouped first. The first group is given a space-time difference based on the centroid (average) of the space-time differences of the two tornadoes. Then the two tornadoes (or the first tornado group centroid and another tornado) with the next smallest  $\delta_k$  are grouped second. The procedure continues by grouping tornado pairs, group-tornado pairs, and group-group pairs until there is a single large group. The grouping is done with the `hclust` function from the `stats` package and it produces the same result as the ST-DBSCAN algorithm (Birant and Kut 2007).

Our interest centers on groups that are not too small (e.g., a family of tornadoes from a single supercell) and not too large (e.g., all tornadoes during a year). So we stop grouping once there are no additional pairs within a  $\delta_k$  of 100K. This stopping threshold of 100K results in 4,638 tornado groups with 2,182 groups containing only one tornado. Also, there are 198 groups with at least 30 tornadoes (which we call ‘large’) with the largest group having 390 tornadoes over seven days. The longest (April 22–28, 2011) event within our largest group had a duration of nine days and produced 360 tornadoes. Roughly 82% of our large groups have a duration of two, three, or four days. There are only nine large groups that are not multi-day events.

#### *b. Comparison of groups with well-known outbreaks*

We compare the tornado groups identified with our objective method with outbreaks that were identified using more subjective criteria. In particular, we focus the comparison on multi-day outbreaks as identified in Forbes (2004). Forbes (2004) (hereafter F04) provides a list of the top 25 outbreaks by number of tornadoes between 1925 and 2004. Only 13 of the outbreaks identified by F04 occur after 1994; the start year of our analysis. The two lists match fairly well (Table 1). We identify ten of F04’s top 13 although the date ranges do not match

identically. For example, the May 18–19, 1995 outbreak identified by F04 is identified by our grouping from May 15–19, 1995. F04 identifies three outbreaks over the common period covered by both studies that are not identified in our top 13 including those that occurred May 15–16, 2003, November 9–11, 2002, and April 19–20, 1996. These outbreaks show up on our list ranked by number of tornadoes at 29, 43, and 41, respectively. We identify five groups in our top 13 that are not mentioned in F04. We perfectly match the top 3 tornado outbreaks identified by Fuhrmann et al. (2014) using 100K. Additionally, Schneider et al. (2004) identifies our top group (May 3 – May 11, 2003) using a subjective clustering method.

**Table 1:** Top 13 tornado groups and outbreaks over the common period of analysis using 100K space-time differences as the cutoff threshold for including tornadoes.

Our Top 13 Groups	Forbes’ Top 13 Outbreaks
<b>May 3-11, 2003*</b>	<b>May 29 – 31, 2004*</b>
<b>May 28-31, 2004*</b>	<b>Jan 21-22, 1999*</b>
<b>Jan 21-22, 1999*</b>	<b>May 3-4, 1999*</b>
<b>May 2-4, 1999*</b>	<b>May 6-8, 2003*</b>
<b>May 15-19, 1995*</b>	<b>May 4-5, 2003*</b>
<b>Jun 22-24, 2003*</b>	<b>Sep 5-8, 2004*</b>
Jun 3-6, 1999	<b>Jun 24, 2003*</b>
Sep 15-18, 2004	<b>Nov 23-24, 2004*</b>
Apr 25-28, 1994	<b>May 9-11, 2003*</b>
May 24-28, 1997	May 15-16, 2003
<b>Nov 22-24, 2004*</b>	Nov 9-11, 2002
<b>Sep 4-8, 2004*</b>	Apr 19-20, 1996
May 30-June 2, 1998	<b>May 18-19, 1995*</b>

**\* indicates a match**

We quantify the percent agreement between our groups and the outbreaks identified in F04 as follows. We count the total number of opportunities for a match as  $13 + 13 = 26$ . We then subtract from this total the number of miss matches ( $3 + 5$ ) and divide by the total opportunities expressing the fraction as a percentage agreement. Here the agreement is 69% [ $(26 - 8)/26 * 100\% = 69\%$ ]. By varying the stopping threshold in the cluster algorithm, we change the percent agreement (Fig. 1). We vary the stopping threshold in increments of 25K over the range of space-time differences from 150K to 25K and find the best match with F04 in terms of percent agreement at 85% when the threshold is 50K. We use 50K

as the stopping threshold for further analysis because it provides the best agreement with F04. This smaller space-time difference results in 6,899 unique groups and 137 large (at least 30 tornadoes) groups. The largest group is the April 26 – April 28, 2011 event that produced 292 tornadoes. The duration of the groups range from 49 one-day events to one five-day event. Multi-day events account for 64% of our large groups.

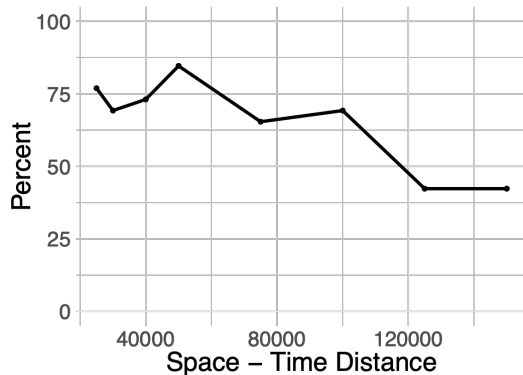


**Figure 1:** Percent agreement between our tornado groups and the tornado outbreaks identified in Forbes (2004).

### c. Big Days in Large Groups

Our objective is to quantify the extent to which the well-known environmental factors statistically explain tornado activity. Since some of the environmental factors have large diurnal fluctuations that can confound a multi-day analysis, we reduce our focus further by considering only the most prolific (big) days in these largest groups. We define the day as the 24-hour period starting at 6 AM local time (often referred to as the ‘convective’ day) (Doswell et al. 2006). A big convective day as part of a large group is defined as one with at least ten tornadoes.

With this definition, we find 177 big days within our large groups. Note that there are sometimes more than one big day in a single large group. Also, big days can occur within smaller groups, and our set of big days accounts for only 25% of all big days in the dataset. The top two big days are associated with the largest tornado group occurring on April 26, 2011 and April 27, 2011 (Table 2).

**Table 2:** The top ten big days in the largest tornado groups.

Convective Day	Number of Tornadoes	Number of Casualties
Apr 27, 2011	173	3069
Apr 26, 2011	103	97
Jan 21, 1999	99	171
Jun 24, 2003	94	12
May 5, 2007	90	24
May 25, 2011	90	23
May 30, 2004	88	46
May 4, 2003	86	384
Feb 5, 2008	85	482
Apr 14, 2012	84	79

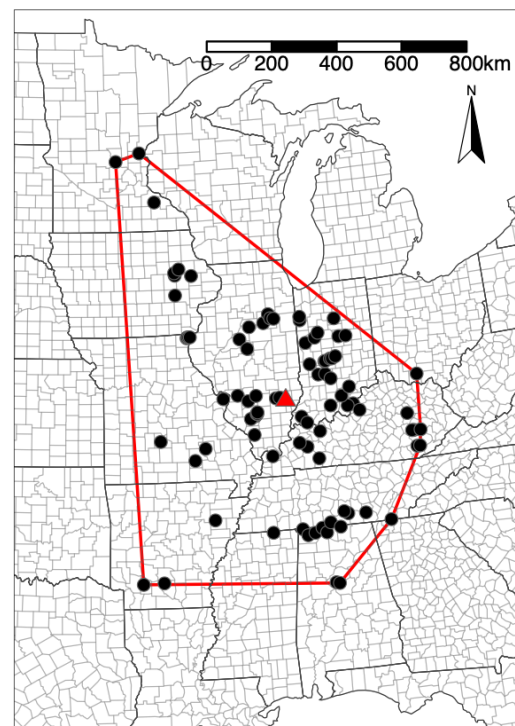


**Figure 2:** The May 30, 2004 big tornado day is characterized by 88 tornadoes. Each dot represents a tornado genesis location, and the triangle is the geographic center of the genesis location. The dark gray line defines the minimum convex polygon around the genesis locations (convex hull).

We use the May 30, 2004 as an example of a big day within a large group. The large group was identified as the second most prolific by our method (and the first most prolific by Forbes (2004) and extended over a four-day period beginning on May 28th. This is the seventh biggest convective day as defined by the

number of tornadoes in any large group identified. Figure 2 shows the genesis locations of the 88 tornadoes on that day. The gray triangle is the geographic center of the set of genesis locations (centroid) and the gray polygon defines the minimum convex area encompassing all locations (convex hull) on the day.

#### d. Accumulated Tornado Energy

We use tornado counts to define our tornado groups because this is what other researchers have done to define outbreaks. But, our interest in this study is on the collective amount of energy all the tornadoes dissipate on big days. The standard measure of tornado intensity is the Fujita and Enhanced Fujita scales (Malamud and Turcotte 2012), but tornado path length and width are often used to compute other intensity metrics (Brooks 2003; Fuhrmann et al. 2014; Malamud and Turcotte 2012). Over a group of tornadoes, the Destructive Potential Index (DPI) is used as a metric of the potential for damage and casualties (Thompson and Vescio 1998). Additional collective measures of intensity, such as the adjusted Fujita mile, measure the outbreak strength by using the EF scale rating times the path length of the tornado (Fuhrmann et al. 2014).

The energy dissipation ( $E$ ) of a tornado estimates the potential wind energy lost at the ground. It represents the potential for destruction in units of power (watts) and is calculated using damage path area ( $A_p$ ), air density ( $\rho$ ), midpoint wind speed ( $v_j$ ) for each EF rating ( $j = 0, \dots, J$ , where  $J$  is the maximum EF rating), and the fraction of the damage path ( $w_j$ ) associated with each rating (Fricker et al. 2017). Since  $E$  is an extensive variable, we sum the energy dissipation over all tornadoes occurring on a big day to get the accumulated tornado energy (ATE). Mathematically, we express  $E$  and ATE as

$$E = A_p \rho \sum_{j=0}^J w_j v_j \quad (2a)$$

$$ATE = \sum_{i=1}^n E_i \quad (2b)$$

#### e. Environmental Factors

Given a big day with at least ten tornadoes, we want to quantify the effect of known

environmental factors on accumulated tornado energy (ATE). To do this, we obtain environmental data from the National Climatic Data Centers (NCDC) North American Regional Reanalysis (NARR). We download the 18Z NARR data for each big day. The 18Z data are chosen because tornado activity generally peaks in the early afternoon. The NARR dataset ends in September 2014 so we use only the big days that occur between January 1994 and September 2014. This includes 154 big days.

Each NARR file has 434 atmospheric variables. We consider five of them representing instability and wind shear including the 0 to 180 mb CAPE and CIN (layer 375, 376), the 0 to 3000 m helicity (layer 323), and the 0 to 6000 m U and V components of storm motion (layer 324, 325). We compute bulk shear as the square root of the sum of the velocity components squared. We use these variables because they are known to be associated with tornado development (Brown 2002; Jackson and Brown 2009; Craven et al. 2002).

Values for each NARR variable on each big day are available as a 277 by 349 rectangular raster. The corresponding big day convex hull is used as a mask, and the raster values falling under the mask are composited into a single number. For the variables CAPE, bulk shear, and helicity, the composite consists of taking the maximum value across all values under the mask. For CIN, the composite consists of taking the minimum value. In this way, every big day value for ATE is associated with each of the four environmental variables representing a spatial composite of the regional scale environment in which the tornadoes occurred. The maximum (or minimum) are chosen for the composite value to insure the variable is a sample from only the unstable airmass.

### 3. Results

#### a. Big Day Climatology

For each big day in a large group, we calculate the centroid from the tornado genesis locations. Figure 3 shows the centroids of all 177 big days in large tornado groups with the size of the triangle scaled by the number of tornadoes in the group. Most of the big days occur east of Rockies and west of the Appalachians. In particular, there is a cluster of centroids across the middle South extending northwestward



toward the central Great Plains. There is a tendency for the biggest days to occur farther east. The centroids do not have an obvious population bias.

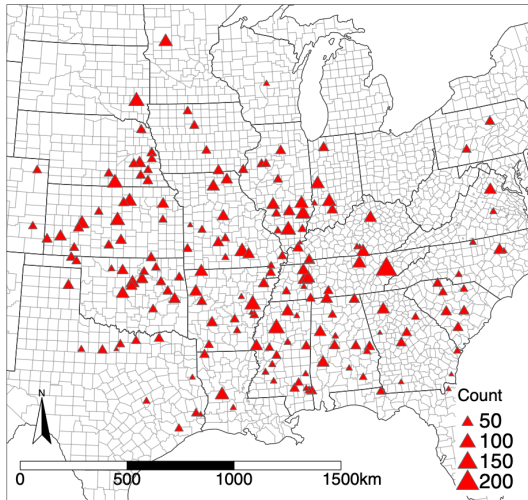


**Figure 3:** Centroids of genesis locations occurring on big days in large groups. The triangles are sized by the number of tornadoes on that day.

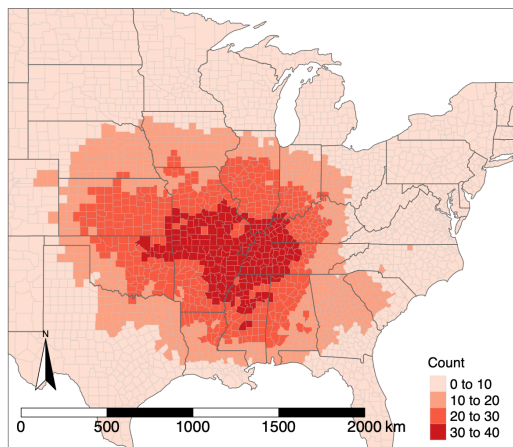


**Figure 4:** Big day density by county.

A convex hull is obtained for each big day. The convex hull represents the spatial domain of tornado activity on that day. Counties within the hull define the political extent of the activity, and we tally the number of times each county falls within (including partially) a big day hull (Figure 4). Of course, larger counties will have a higher count considering all else being equal, but a pattern emerges highlighting the counties over the middle South. Counties affected most often

by big days in large groups include those of northeastern Oklahoma eastward across southern Missouri and northern Arkansas into western Kentucky and western Tennessee.

*b. Accumulated Tornado Energy*

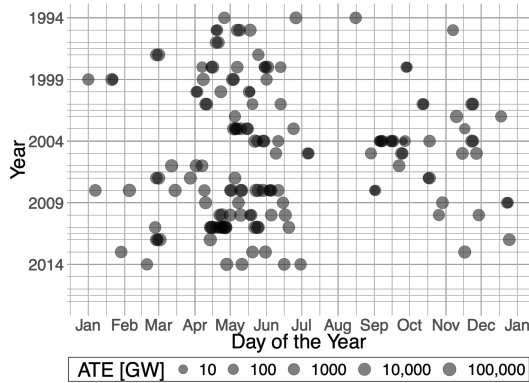
Table 3 lists in rank order the big days in the largest groups by ATE. It includes the infamous days of April 27, 2011 and May 4, 2003. ATE on April 27, 2011 is nearly four times the ATE on the next most energetic day. April 26, 2011 ranks third. Over all big days, the Spearman rank correlation between ATE and the number of tornadoes is .67 indicating a strong relationship.

**Table 3:** Top ten convective days ranked by accumulated tornado energy (ATE) in units of terawatts (TW).

Convective Day	ATE (TW)
Apr 27, 2011	221
Apr 24, 2010	64
Apr 26, 2011	46
May 24, 2011	43
Feb 5, 2008	39
Mar 2, 2012	38
May 10, 2010	34
Apr 14, 2012	32
May 4, 2003	31
May 22, 2004	30

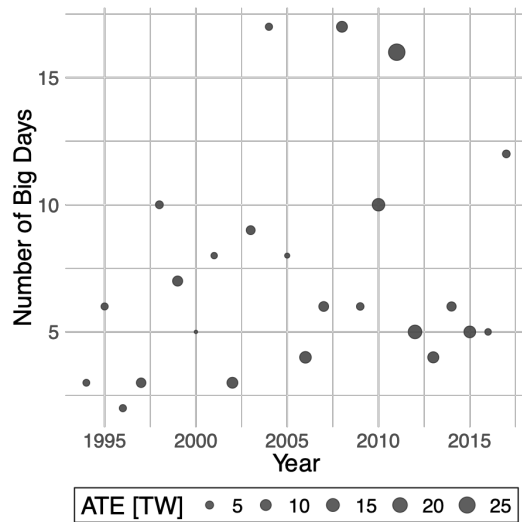
**Table 4:** Seasonal variation in ATE (TW), number of tornadoes, and number of prolific days by month. The number of tornadoes and number of big days are based on the period 1994 – 2017.

Month	Average ATE (TW)	Number of Tornadoes	Number of Big Days
January	4.07	345	7
February	7.89	321	9
March	13.58	427	10
April	16.24	1696	37
May	8.92	2220	49
June	4.10	729	18
July	0.63	43	2
August	1.47	71	2
September	1.01	458	16
October	2.28	261	8
November	8.11	587	14
December	5.59	123	5



**Figure 5:** Accumulated tornado energy (ATE) by day of year on days with more than ten tornadoes occurring within large groups of at least 30 tornadoes, 1994-2017. Tic labels on the x-axis are the start day of each month.

Big days within large groups are most likely to occur during April through June with some years also showing a secondary peak after summer (Fig. 5). Monthly average ATE peaks in April followed by March and May (Table 4). Average ATE is higher during November than during May. While fewer in number, big days in large groups during November tend to produce stronger tornadoes.



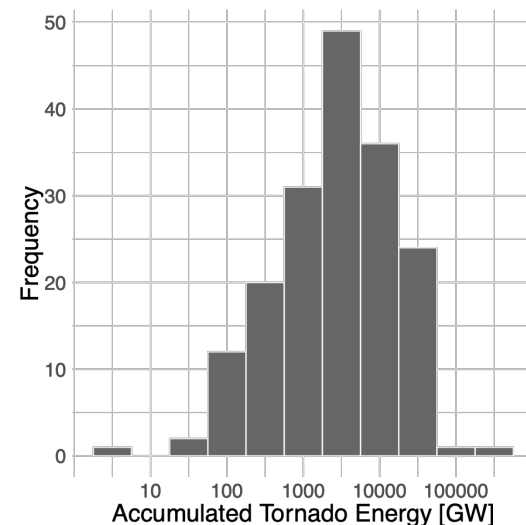
**Figure 6:** Number of big days by year, 1994-2017. Points are sized by annual average ATE.

Fig. 6 shows the time series of the annual number of big days in large groups and the annual average ATE over those days. The inter-annual variation in the number of big days is quite large ranging between two and 37, but there

is no long-term trend. On the other hand, the annual average ATE appears to be increasing with the higher values occurring later in the period.

*c. Quantifying the Relationship Between ATE and Environmental Factors*

With our sample of 154 big days from 1994 – September 2014, we use a regression model to quantify the relationships between ATE and regional scale environmental factors. A multiple regression model allows us to quantify, for example, the effect of CAPE on ATE while controlling for time of year. We use month as an index for time of year, and it is included in the model as a random offset to the intercept term. Environmental variables are considered fixed effects as is year. The coefficient on year is the annual trend. Values of ATE are skewed to the right with most big days having less than 5 TW. However, the top ten days have more than 30 TW each with the top day having more than 220 TW (see Table 3). The distribution of ATE on a log scale is nearly symmetric about the mean value of 9 TW (Fig. 7). The median value is 3.2 TW, and the geometric mean is 2.6 TW. So, the model uses the logarithm of ATE as the response variable.



**Figure 7:** Histogram of per big day ATE, 1994-2017. The horizontal axis is on a log scale.

We examine various combinations of the fixed effects and find that the best model for ATE is

$$\ln(\text{ATE}) = \beta_0 + \beta_{\text{Year}} \text{Year} + \beta_{\text{CAPE}} \text{CAPE} + \beta_{\text{Shear}} \text{Shear} + \beta_{\text{Month}}(1|\text{Month}) \quad (3)$$

where the coefficients for these terms are given by the corresponding  $\beta$ 's. Helicity and CIN do not improve the model fit. The model is best in the sense that it has the lowest value of AIC. The in-sample correlation between ATE and model predicted ATE is .54.

**Table 5:** Coefficient estimates from a regression model of ATE onto year, CAPE, and shear using data from  $n = 154$  big days in large groups over the period January 1994 through September 2014. Std. Error is the standard error of the estimate and the  $t$  value is the ratio of the estimate to the standard error. The coefficients were determined via an interactive maximum likelihood approach with the `lmer` function from the `lme4` package for R (Bates et al. 2015).

	Estimate	Std. Error	$t$ value
$\beta_0$	25.609	0.656	39.060
$\beta_{\text{Year}}$	0.079	0.022	3.520
$\beta_{\text{CAPE}}$	0.396	0.118	3.355
$\beta_{\text{Shear}}$	0.606	0.205	2.954

Model coefficients are given in Table 5. We interpret them as follows. The coefficient on the year term ( $\beta_{\text{Year}}$ ) indicates an upward trend in per big-day outbreak ATE (see Fig. 6) amounting to 7% [(2.5%, 12%), 95% uncertainty (confidence) interval (UI)] per annum. Note that the percent increase is calculated using  $(e^{\beta_{\text{Year}}} - 1) \times 100\%$ . The coefficient on the CAPE ( $\beta_{\text{CAPE}}$ ) term indicates that for every 1000 J kg<sup>-1</sup> increase in CAPE, ATE increases by 49% [(18%, 87%), 95% UI] holding the other variables constant. The coefficient on the bulk shear term ( $\beta_{\text{Shear}}$ ) indicates that for every 10 m<sup>2</sup> s<sup>-2</sup> increase in the magnitude of bulk shear, ATE increases by 83% [(23%, 174%), 95% UI] holding the other variables constant.

#### d. Model residuals

We compute the conditional standardized residuals (Santos Nobre and da Motta Singer 2007) between the actual and predicted values of ATE. The histogram of the residuals can be described by a normal distribution, and a plot of the residuals as a function of the predicted

values by month shows no apparent pattern (Fig. 8) indicative of an adequate model.

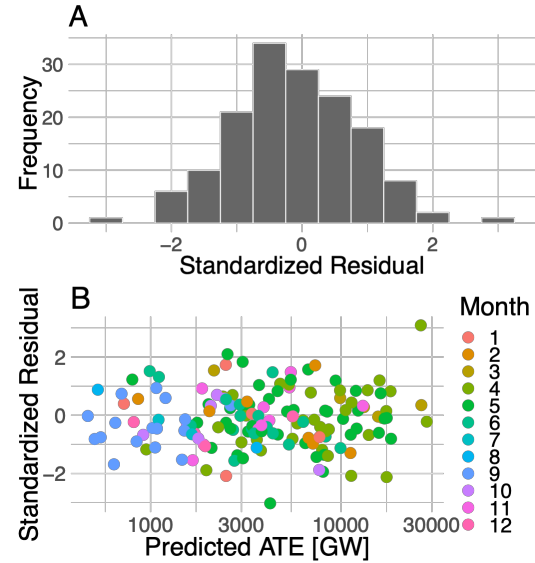


**Figure 8:** Conditional standardized residuals from the linear regression model. (A) Histogram and (B) Residuals as a function of predicted values of ATE.

Figure 9 shows the actual ATE versus predicted ATE for the 154 big tornado days. Lighter blue points, which tend to cluster toward greater ATE, indicate more tornado casualties (deaths plus direct injuries). The points tend to fall along a line from lower left to upper right but with a slope less than one.

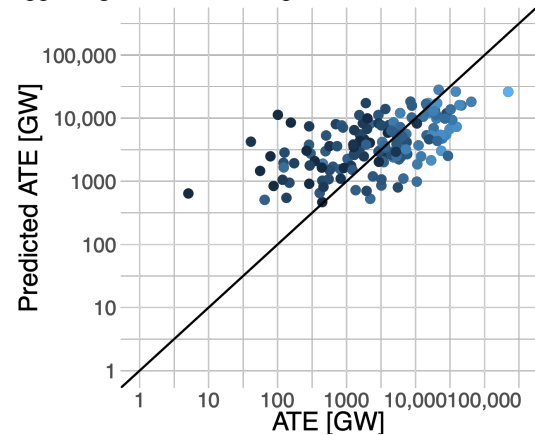


**Figure 9:** Actual versus predicted accumulated tornado energy (ATE) for the  $n = 154$  big tornado days. The predicted are based on the regression model (Eq. 3). The color shading from dark to light indicates increasing number of casualties.



Big days with more ATE than predicted by the model are the points that fall to the right of the diagonal line. We note that April 27, 2011 and May 22, 2004 are examples of days more energetic than predicted by the model, and April 19, 2011 and May 18, 2000 are examples of days less energetic than predicted by the model. Figure 10 shows the polygons defining boundaries of the tornadoes on days when the model most over predicted ATE and on days when the model most under predicted ATE. We see no geographic preference for big days that are under predicted compared with big days that are over predicted. Further, we see no distinction in the size of the areas.

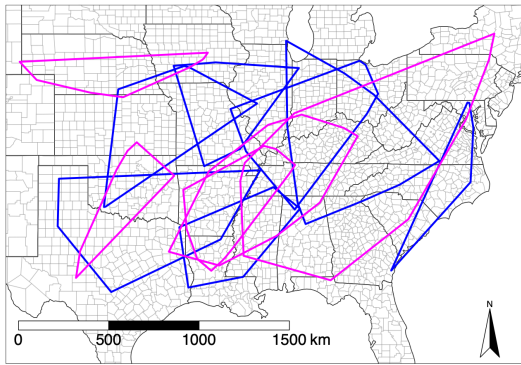


**Figure 10:** Areas defining the boundary of all tornadoes on big days. Days selected are those where the model most over predicted (blue) and most under predicted (pink) ATE.

On the other hand, the average number of tornadoes per unit area on the subset of the big days that are most under predicted is 3.5 per square kilometer compared to 1.5 per square kilometer on the subset of the big days that are most over predicted. This implies that the model might be improved by including an environmental factor that explains the efficiency of tornado production. More research on this is needed.

#### 4. Summary and List of Major Findings

April 27, 2011 was the biggest day in the largest, costliest, and one of the deadliest tornado outbreaks ever recorded in the United States (Knox et al. 2013). The multi-day event affected 21 states from Texas to New York. In this study, we first identify all big days over the period 1994–2017 having ten or more tornadoes that occur in multi-day groups having

30 or more tornadoes (large groups). This is done with a cluster technique on the set of space-time differences between all tornadoes. Then, for each big day, we compute the accumulated tornado energy (ATE) as the sum total of the energy dissipated over all tornadoes on that day. Next, we use reanalysis grids to identify the extremes in CAPE, CIN, bulk shear, and helicity over the domain defined by the tornado locations on these big days. A regression model is used to quantify the relationship between ATE and the four environmental factors. We find an upward trend in ATE at the rate of 7% per annum. We also find that ATE increases significantly with additional CAPE and bulk shear but not with helicity. Finally, residuals are analyzed to diagnose model adequacy and to identify the largest under and over predictions.

The major findings are:

- An objective cluster technique can reliably identify tornado outbreaks
- Accumulated tornado energy is a useful metric of outbreak severity.
- Outbreak severity increases by 49% for every  $1000 \text{ J kg}^{-1}$  increase in CAPE.
- Outbreak severity increases by 83% for every  $10 \text{ m}^2 \text{ s}^{-2}$  increase in bulk shear.

The study is limited by sample size (only 154 big day cases) and by an exclusive focus on the last 20 years of a much longer tornado record. The study could be improved by considering more cases from the earlier years. The cost of including earlier data would be greater uncertainty on the estimates of per-tornado energy dissipation. The study might also be improved by including other environmental factors in the model, especially ones that are related to the efficiency of tornado production. Future work will examine the spatial variation in the factors affecting outbreak severity and quantify the relationship between outbreak casualties and the environmental factors controlling for how many people were within the outbreak area.

#### ACKNOWLEDGEMENTS

The code used to produce the results of this paper is available at <https://github.com/jelsner/tor-clusters>

#### REFERENCE

- American Meteorological Society, cited 2018: Tornado Outbreak. Glossary of Meteorology. [Available online at [http://glossary.ametsoc.org/wiki/Tornado\\_outbreak](http://glossary.ametsoc.org/wiki/Tornado_outbreak).]
- Bates, D., M. Mächler, E. Zurich, B. M. Bolker, and S. C. Walker, Fitting Linear Mixed-Effects Models Using lme4. *Journal of Statistical Software*, 67(1), 1 - 48.
- Birant, D., and A. Kut, 2007: ST-DBSCAN: An algorithm for clustering spatial-temporal data. *Data Knowl. Eng.*, **60**, 208–221,.
- Brooks, H. E., 2003: On the Relationship of Tornado Path Length and Width to Intensity. *Weather and Forecast.*, **19**, 310–319,.
- , C. A. Doswell, and J. Cooper, 1994: On the Environments of Tornadoic and Nontornadoic Mesocyclones. *Weather Forecast.*, **9**, 606–618,.
- Brown, M., 2002: The Spatial, Temporal, and Thermodynamic Characteristics of Southern-Atlantic United States Tornado Events. *Phys. Geogr.*, **23**, 401–417,.
- Concannon, P. R., H. E. Brooks, and C. A. D. III, 2000: Climatological Risk of Strong and Violent Tornadoes in the United States. *2nd Conf. Environ. Appl.*,.
- Craven, J. P., R. E. Jewell, and H. E. Brooks, 2002: Comparison between observed convective cloud-base heights and lifting condensation level for two different lifted parcels. *Weather Forecast.*, **17**, 885–890,.
- Dean, A. R., An Analysis of Clustered Tornado Events. *25<sup>th</sup> Conference on Severe Local Storms*.
- Doswell, C. a., R. Edwards, R. L. Thompson, J. a. Hart, and K. C. Crosbie, 2006: A Simple and Flexible Method for Ranking Severe Weather Events. *Weather Forecast.*, **21**, 939–951,.
- Forbes, G. S., 2004: Meteorological Aspects of High-Impact Tornado Outbreaks. Preprints, *22<sup>nd</sup> Conf. on Severe Local Storms*, Hyannis, MA, Amer. Meteor. Soc., 1 - 12.
- Fricker, T., J. B. Elsner, and T. H. Jagger, 2017: Population and energy elasticity of tornado casualties. *Geophys. Res. Lett.*, **44**, 3941–3949,.
- Fuhrmann, C. M., C. E. Konrad, M. M. Kovach, J. T. McLeod, W. G. Schmitz, and P. G. Dixon, 2014: Ranking of Tornado Outbreaks across the United States and Their Climatological Characteristics. *Weather Forecast.*, **29**, 684–701,.
- Galway, J. G., 1977: Some Climatological Aspects of Tornado Outbreaks. *Mon. Weather Rev.*, **105**, 477–484,.
- Jackson, J. D., and M. E. Brown, 2009: Sounding-Derived Low-Level Thermodynamic Characteristics Associated with Tornadoic and Non-Tornadoic Supercell Environments in the Southeast United States. *Natl. Weather Dig.*, **33**, 16–26.
- Johns, R. H., J. M. Davies, and P. W. Leftwich, 1993: Some wind and instability parameters associated with strong and violent tornadoes: 2. Variations in the combinations of wind and instability parameters. American Geophysical Union (AGU), *Geophysical Monograph Series*, 583–590.
- Knox, J. A., and Coauthors, 2013: Tornado debris characteristics and trajectories during the 27 april 2011 super outbreak as determined using social media data. *Bull. Am. Meteorol. Soc.*, 1371–1380,.
- Knupp, K. R., and Coauthors, 2014: Meteorological overview of the devastating 27 april 2011 tornado outbreak. *Bull. Am. Meteorol. Soc.*, **95**, 1041–1062,.
- Korotky, W., R. W. Przybylinski, and J. A. Hart, 1993: The Plainfield, Illinois, tornado of August 28, 1990: The evolution of synoptic and mesoscale environments. American Geophysical Union (AGU), *Geophysical Monograph Series*, 611–624.
- Malamud, B. D., and D. L. Turcotte, 2012: Statistics of severe tornadoes and severe tornado outbreaks. *Atmos. Chem. Phys.*, **12**, 8459–8473,.
- Malamud, B. D., D. L. Turcotte, and H. E. Brooks, 2016: Spatial-temporal clustering of tornadoes. *Nat. Hazards Earth Syst. Sci.*, **16**, 2823–2834, doi:10.5194/nhess-16-2823-2016,.
- Santos Nobre, J., and J. da Motta Singer, 2007: Residual Analysis for Linear Mixed Models. *Biometrical J.*, **49**, 875–875,.
- Schneider, R.S., Brooks, H.E., & Schaefer, J. T.,

2004: Tornado Outbreak Day Sequences: Historic Events and Climatology (1875-2003). *Prepr. 22d Conf. Sev. Local Storms, Hyannis, MA, Amer. Meteor. Soc.*, **2003**, 3-8.

Thompson, R. L., and M. D. Vescio, 1998: The Destruction Potential Index - A Method for Comparing Tornado Days. *19th Conf. Sev. Local Storms,*